Available online at www.sciencedirect.com
ScienceDirect
Ceramics International 38 (2012) 995–1002
CERAMICS INTERNATIONAL
www.elsevier.com/locate/ceramint

Improvements on the mechanical properties and thermal shock behaviours of MgO–spinel composite refractories by ZrO_2 incorporation

Rasim Ceylantekin [1], Cemail Aksel *

Department of Materials Science and Engineering, Anadolu University, Iki Eylul Campus, Eskisehir 26470, Turkey

Received 3 June 2011; received in revised form 3 August 2011; accepted 8 August 2011
Available online 17 August 2011

Abstract

Microstructural features and improvements on the mechanical properties and thermal shock behaviours of MgO–spinel composite refractories with ZrO_2 addition were examined. ZrO_2 incorporation into MgO–spinel led to improvements around ~1.5-fold ratios on mechanical properties, R_{st} values and thermal shock results. The basic parameters improving mechanical properties and thermal shock resistance of MgO–spinel–ZrO_2 composite refractories were determined as follows: (i) propagation of microcracks for a short distance by interlinking each other, (ii) stopping or deviation of microcracks when reaching pores or ZrO_2 particles, (iii) concurrent occurrence of mostly intergranular and some transgranular cracks on fracture surfaces, and with the addition of ZrO_2 (iv) the increase in bulk density, and (v) a significant decrease in MgO grain size. The improvements observed in thermo-mechanical properties confirmed that MgO–spinel–ZrO_2 refractories showed a low strength loss and high thermal shock damage resistance at high temperatures, leading to longer service lives for using industrial applications.

Keywords: C. Mechanical properties; C. Thermal shock resistance; $MgAl_2O_4$; Zirconia

1. Introduction

There are no natural deposits of magnesium aluminate spinel ($MgAl_2O_4$), which is therefore normally obtained by reaction of mixtures of magnesium and aluminium oxides. Spinel is an important constituent of MgO-based refractory materials. The main application areas of spinel refractories are transition and burning zones of cement rotary kilns, side walls and bottom of steel teeming ladles and checker work of glass tank furnace regenerators [1–3]. The most important factor in MgO–spinel refractories' being used prevalently among the other MgO and dolomite originated refractory materials is their much higher resistance to thermal shocks and alkali attacks [2,4,5]. In MgO–chrome refractories, concerns on allergy, ulcer and carcinogen effects on skin of the toxic Cr^{6+} ions obtained from Cr_2O_3 have led to the need for use of no-chromium containing alternative MgO–spinel refractories [6]. The MgO–spinel refractories have a service life of ~1.5–2 times longer than MgO–chrome refractories [7]. MgO–spinel bricks are preferred in the cooling and transition zones where thermal stresses occur due to high temperature difference and therefore severe thermal shocks during cooling and heating in cement rotary kilns [1]. In addition, their use in the sintering zone that requires strength and high temperature affords economic benefits [1]. MgO–spinel refractories are preferred as they display high thermal shock resistance in areas requiring strength at high temperatures and also due to their high resistance against basic slag, alkali attacks and molten metal abrasions [4]. Furthermore, stoichiometric spinel used as lining in alumina originated ladles and cement rotary kilns shows high resistance against the corrosion and abrasion caused by calcium–aluminium–silicate containing constituents [7].

The additions of spinel to MgO and additives to MgO–spinel improve the retained strength after thermal shock, hot modulus of rupture, refractoriness under load and densification characteristics of these composite refractories [2–4,8–10]. Although service life of MgO–spinel refractories is prolonged especially in connection with the increase in work of fracture energy by incorporation of spinel particles into MgO, a reduction occurs in other mechanical properties [11–14]. This study has been conducted for further improving the mechanical

* Corresponding author. Tel.: +90 222 3350580x6362; fax: +90 222 3239501.
E-mail address: caksel@anadolu.edu.tr (C. Aksel).
[1] Present address: Department of Ceramic Engineering, Dumlupınar University, Merkez Campus, Kutahya 43100, Turkey.

0272-8842/$36.00
doi:10.1016/j.ceramint.2011.08.022

and thermal shock performances of materials and further prolonging service life by obtaining high thermo-mechanical properties as a result of the increase in resistance to fracture by addition of zirconia in different proportions to MgO–spinel composite refractories containing various quantities of $MgAl_2O_4$ spinel. The relationships between mechanisms affording improvement on the mechanical and thermal shock behaviours of refractories and microstructural changes and parameters affecting these have been examined in detail with reasons.

2. Materials and methods

Recipes were prepared by adding weight of zirconia (ZrO_2) in proportions of 5%, 10%, 20% and 30% to compositions obtained by adding 5%, 10%, 20% and 30% $MgAl_2O_4$ spinel (S) by weight to MgO (M), as given in Table 1. Batches prepared using MgO (0–1 mm), spinel (0–1 mm) and zirconia (~2.5 μm) were shaped into samples of ~8 mm × 8 mm × 60 mm applying ~100 MPa pressure. The samples were sintered for 2 h in kiln (Nabertherm HT16/18) at 1600 °C using 5 °C/min heating and cooling rates. Bulk density and apparent porosity values of 3 specimens from each composition were measured using the standard water immersion method and average values were taken [15]. After samples were ground using 800 and 1200 grade SiC papers until obtaining smooth surfaces based on the standard sample preparation rules [13,16], the samples were dried at ~110 °C in an oven and mechanical tests were carried out. The mechanical tests performed using a load cell of 2 kN moving at a velocity of 0.5 mm/min with support roller span (L) of 40 mm were applied to minimum 5–6 samples and average values were taken. Under standard tests, values of strength [16] $\{\sigma = (3/2)(PL)/(WD^2)\}$, modulus of elasticity [17] $\{E = L^3m/(4WD^3)\}$, fracture toughness [18–21] $\{K_{1C} = (3/2)(PLc^{1/2}Y)/(WD^2)\}$ and fracture surface energy, γ_S [22], $\{K_{1C} = (2E\gamma_S)^{1/2}\}$ were determined by the 3-point bending method in Instron 5581. K_{1C} and γ_S measurements were carried out using Single Edge Notched Beam (SENB) method. The parameters used in those equations given above are as follows [16–22]: P is the load at failure, W is the specimen width, D is the specimen thickness, m is the slope of the tangent of the initial straight-line portion of the load-deflection curve, c is the notch depth, and Y is a dimensionless constant that depends on the geometry of the loading and the crack configuration, $\{Y = A_0 + A_1(c/D) + A_2(c/D)^2 + A_3(c/D)^3 + A_4(c/D)^4\}$, for $L/D \sim 8$, $A_0 = 1.96$, $A_1 = -2.75$, $A_2 = 13.66$, $A_3 = -23.98$, $A_4 = 25.22$. The magnitude of critical defect size (C) value was calculated using Griffith equation [22–26], where combining the SENB fracture toughness values with those of strength allowed an estimate to be made of the critical defect size [13,27]. E values were calculated based on the slope of stress–strain curve in the initial linear portion of the curve between lower and upper bounds, where the steepest slope was reported as the modulus [12,17]. K_{1C} and γ_S values were calculated by using notches at a depth of ~25% of thickness (~2 mm) of the material using a diamond disk 700 μm thick on specimens. Notch depth was measured using an Olympus BX60M brand optical microscope. X-ray diffraction (XRD) analysis was performed using Rigaku RINT2000 equipment. SEM studies were carried out using Zeis Evo 50 device with the microstructures and fracture surfaces of materials analyzed. Using photographs taken on the surfaces of specimens, which were polished and thermally etched for 10 min at 1450 °C, the average MgO grain size was calculated using standard equation employing a standard line mean intercept method [28] ($D = 1.56L$, D is the average grain size, L is the average intercept length). The R_{st} thermal shock parameter values, which represents the maximum temperature difference allowed required for propagation of long cracks under severe thermal stress conditions, used in estimating the further weakening and crack stability of the composite refractory materials with the increase in the severity of thermal shock were calculated by the following formula [29]: $\{R_{st} = [\gamma_S/(\alpha^2.E)]^{1/2}\}$, where α is the mean thermal expansion coefficient of the composite refractory. Thermal shock tests were performed through sudden cooling in water from 500 and 1000 °C to 25 °C room temperature with strength values determined in connection with thermal shock temperatures. The relationships between the obtained data and microstructural changes were investigated in detail with parameters affecting them analyzed.

Table 1
Compositions prepared for mechanical testing where weights of MgO (0–1 mm), spinel (0–1 mm) and ZrO_2 (~2.5 μm) were used.

Compositions	MgO (%)	Spinel (%)	ZrO_2 (%)
M	100	–	–
M–5%S	95	5	–
M–10%S	90	10	–
M–20%S	80	20	–
M–30%S	70	30	–
M–5%S–5%ZrO_2	90	5	5
M–5%S–10%ZrO_2	85	5	10
M–5%S–20%ZrO_2	75	5	20
M–5%S–30%ZrO_2	65	5	30
M–10%S–5%ZrO_2	85	10	5
M–10%S–10%ZrO_2	80	10	10
M–10%S–20%ZrO_2	70	10	20
M–10%S–30%ZrO_2	60	10	30
M–20%S–5%ZrO_2	75	20	5
M–20%S–10%ZrO_2	70	20	10
M–20%S–20%ZrO_2	60	20	20
M–20%S–30%ZrO_2	50	20	30
M–30%S–5%ZrO_2	65	30	5
M–30%S–10%ZrO_2	60	30	10
M–30%S–20%ZrO_2	50	30	20
M–30%S–30%ZrO_2	40	30	30

3. Results and discussion

The results of physical and mechanical properties of composite refractories produced by incorporating varied ratios of zirconia (ZrO_2) into MgO–spinel (M–S) materials containing varied amounts of spinel ($MgAl_2O_4$) were presented below, where their compositions were given in Table 1. The additives

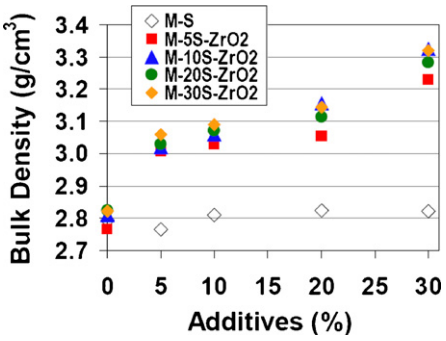

Fig. 1. Bulk density (ρ) as a function of additives (additives: (i) $MgAl_2O_4$ for M–S and (ii) ZrO_2 for M–S–ZrO_2).

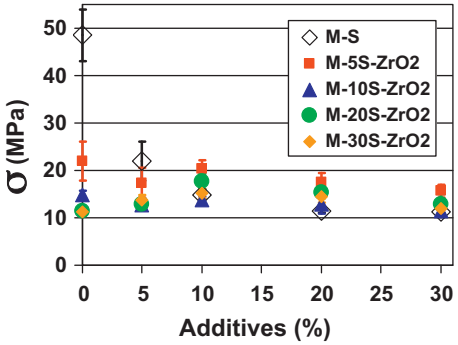

Fig. 3. Strength (σ) as a function of additives (additives: (i) $MgAl_2O_4$ for M–S and (ii) ZrO_2 for M–S–ZrO_2).

used in figures and a table represent: (i) $MgAl_2O_4$ for M–S, and (ii) ZrO_2 for M–S–ZrO_2 materials.

Bulk density (ρ) and apparent porosity results are given in Figs. 1 and 2, respectively. The analysis of the bulk density and apparent porosity results of produced materials shows that the average bulk density values measured for M and M–S refractories are ~2.8 g/cm^3, rising up to ~3.3 g/cm^3 with the addition of increased amounts of ZrO_2. On the other hand, apparent porosity is ~21% in M and M–S materials, demonstrating a decreasing trend down to ~12% as the amount of ZrO_2 added to M–S is increased. Bulk density values have increased significantly with the apparent porosity values decreasing when ZrO_2 used as an additive having a high density [30,31] (ρ_{ZrO_2} : 5.56 g/cm^3) has been incorporated into M–S compositions (ρ_{M-S}: 3.58 g/cm^3).

The results of strength tests of composite refractories produced as a result of addition of ZrO_2 to M–S materials containing varied amounts of spinel were evaluated. Strength (σ) values of 5% ZrO_2 added M–S–ZrO_2 refractories were lower than those of M–S materials; however, when ≥10% ZrO_2 was added to such composites, it was determined that they had higher strength values than that of M–S materials (Fig. 3). The changes occurring in strength values by addition of ZrO_2 to M–30%S and M–5%S compositions where maximum and minimum ratios of spinel were added to MgO were examined. An improvement reaching 33.5% was achieved in M–30% S–ZrO_2 compositions with the addition of ZrO_2. The improvement observed on M–5%S–ZrO_2 compositions is much more distinct. For example, when M–20%S and M–5%S–20%ZrO_2 compositions were compared among the materials containing 20% additives (e.g. including both spinel and ZrO_2), a maximum improvement, which was 1.54-fold, was observed in the strengths of ZrO_2 added composites refractories (Fig. 3).

As shown in Fig. 4, M–S–5%ZrO_2 compositions had lower modulus of elasticity (E) values than that of M–5%S composites. While 10% ZrO_2 containing M–5%S–ZrO_2 composition had a high E value in comparison with M–10%S material, the M–20%S–ZrO_2 composition containing the same amount of ZrO_2 had approximately the same modulus of elasticity data compared to M–10%S material, with the other M–S–ZrO_2 compositions containing 10% ZrO_2 having lower E values than that of M–10%S material. In the modulus of elasticity values of all M–S–ZrO_2 compositions containing 20% and 30% ZrO_2, a marked improvement was observed in comparison with M–S materials containing 20% and 30% spinel (Fig. 4). The improvements observed specifically in M–5%S–ZrO_2 compositions were more distinct and at maximum levels compared to other M–S and M–S–ZrO_2 compositions.

Composite refractories containing both varied ratios of spinel and different amounts of ZrO_2 had higher fracture toughness (K_{1C}) values compared to M–S materials when both spinel and ZrO_2 additives were added at ratios of 10% and

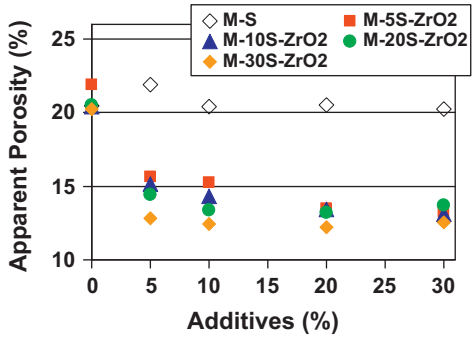

Fig. 2. Apparent porosity as a function of additives (additives: (i) $MgAl_2O_4$ for M–S and (ii) ZrO_2 for M–S–ZrO_2).

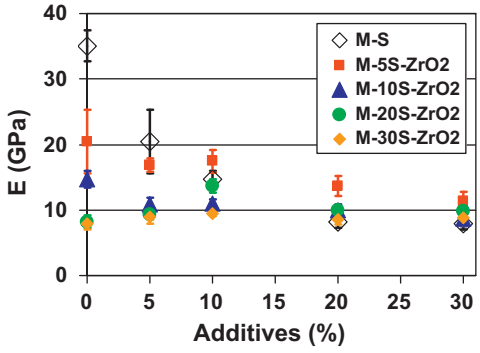

Fig. 4. Modulus of elasticity (E) as a function of additives (additives: (i) $MgAl_2O_4$ for M–S and (ii) ZrO_2 for M–S–ZrO_2).

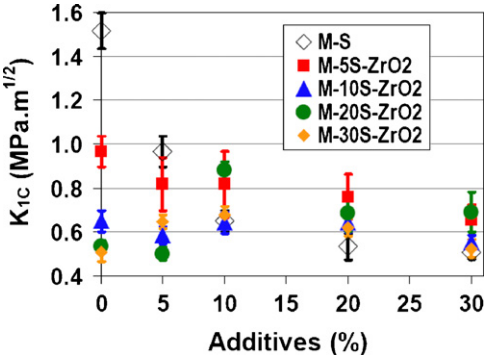

Fig. 5. Fracture toughness (K_{1C}) as a function of additives (additives: (i) $MgAl_2O_4$ for M–S and (ii) ZrO_2 for M–S–ZrO_2).

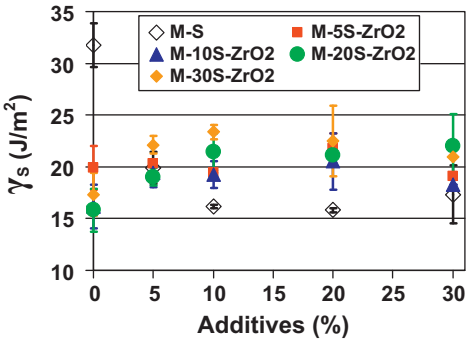

Fig. 7. Fracture surface energy (γ_S) as a function of additives (additives: (i) $MgAl_2O_4$ for M–S and (ii) ZrO_2 for M–S–ZrO_2).

above (Fig. 5). Compositions displaying maximum improvement in their fracture toughness values with the addition of ZrO_2 to M–S materials were examined based on (i) the amount/percentage of added additives (e.g. including both spinel and ZrO_2) and (ii) the amount of ZrO_2 incorporated into M–S composites containing varied ratios of spinel. For example in the composites with 20% additives (containing both spinel and ZrO_2), (i) improvement was at maximum levels with M–5%S–20%ZrO_2 composition showing 1.42-fold higher resistance against resistance to fracture compared to M–20%S material. Furthermore; (ii) the addition of 10%ZrO_2 to M–20%S, as compared to M–20%S material again, led to 1.65-fold improvement, where the highest K_{1C} value was achieved among the M–S–ZrO_2 compositions (Fig. 5).

Critical defect size (C) values as a function of additives are given in Fig. 6. The additions of both spinel to MgO and ZrO_2 to M–S materials enhanced the C values significantly. For example, M–20%S–30%ZrO_2 composition having maximum critical defect size showed marked increases in C values, as compared to both M–30%S and additive-free MgO, by factors of 1.44 and 2.95, respectively. It was observed that the great majority of M–S–ZrO_2 composite refractories had higher C values than those of M–S materials though a few of them had lower critical defect sizes than that of M–S compositions. The rise occurred in C values, where both spinel and ZrO_2 additives were incorporated into MgO, was associated with the improvement in K_{1C} data, showing a high resistance to fracture.

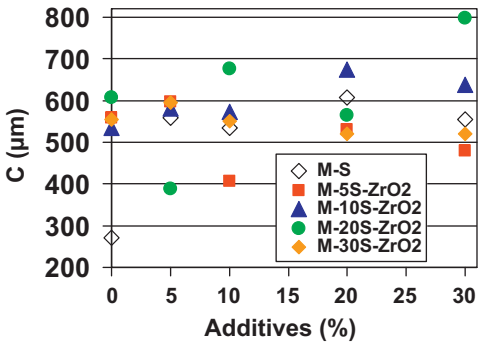

Fig. 6. Critical defect size (C) as a function of additives (additives: (i) $MgAl_2O_4$ for M–S and (ii) ZrO_2 for M–S–ZrO_2).

Fracture surface energy (γ_S) represents the amount of energy required to initiate crack propagation [22]. High γ_S values indicate that more energy is required for initiation of crack propagation and that the initiation of crack propagation will be more difficult and therefore the resistance will be higher compared to low γ_S values. As shown in Fig. 7, the fracture surface energy values of M–S–ZrO_2 composite refractories were significantly higher than those of M–S materials when $\geq$5% additives containing both spinel and ZrO_2 were incorporated. Compositions exhibiting maximum improvement in the fracture surface energy values of ZrO_2 added M–S materials were analyzed based on (i) the amount/percentage of incorporated additives (i.e. both spinel and ZrO_2) and (ii) the amount of ZrO_2 added to M–S refractories containing varied amounts of spinel. In refractories to which 10% additives containing both spinel and ZrO_2 were added, (i) improvement was at maximum levels with M–30%S–10%ZrO_2 refractories displaying a 1.5-fold higher resistance against the initiation of crack propagation in comparison with M–10%S materials. In addition, (ii) incorporation of 10%ZrO_2 into M–30%S composition led to an improvement of 1.4-fold raising γ_S values (Fig. 7). In general, M–30%S–ZrO_2 compositions have higher γ_S values than other compositions, requiring more energy for the initiation of crack propagation. Therefore, the initiation of crack propagation is more difficult compared to other compositions in M–30%S–ZrO_2 refractories and hence resistance is higher. This improvement observed in the fracture surface energy values is also consistent with the below given R_{st} thermal shock parameter and thermal shock results.

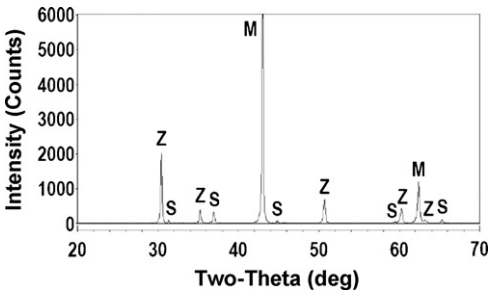

Fig. 8. XRD graph of a composite refractory having M–5%S–20%ZrO_2 composition (M, MgO; S, $MgAl_2O_4$; Z, ZrO_2).

The M–5%S–20%ZrO_2 composite refractory showing significant improvements on mechanical properties for which ZrO_2 was used as an additive in M–S materials was selected as an example. The results of X-ray diffraction (XRD) for M–5%S–20%ZrO_2 composition were given in Fig. 8. According to the phase analysis results; MgO, spinel and cubic zirconia phases were identified in M–S–ZrO_2 composite refractories. In addition, microstructure and the distribution of elements were examined for M–5%S–20%ZrO_2 composite refractory (Fig. 9). The analysis of microstructural images showed that the distribution of used constituents was in general homogeneous. White coloured ZrO_2 particles observed in the microstructure were located predominantly at MgO grain boundaries with some of them located inside the MgO grains. M–S–ZrO_2 composite refractories during cooling after sintering create significant tensile stresses around additives due to the marked difference between the thermal expansion coefficients [30,31] (α) of MgO, spinel and zirconia ($\alpha_{MgO} = 13.6 \times 10^{-6}\,^{\circ}C^{-1}$, $\alpha_{spinel} = 8.4 \times 10^{-6}\,^{\circ}C^{-1}$, $\alpha_{ZrO_2} = 7.6 \times 10^{-6}\,^{\circ}C^{-1}$) and such stresses cause formation of interlinked microcracks [11–14]. It was observed that the microcracks forming in the structure are interlinked to each other and propagate for a short distance and are arrested or display deviation when coming across the ZrO_2 particles or reaching the pores (Fig. 9). In addition, the average MgO grain size was calculated for different compositions picked as examples as (i) pure MgO = 67.2 μm, (ii) M–5%S = 39.8 μm and (iii) M–5%S–20%ZrO_2 = 38.9 μm. As the amounts of additives (i.e. spinel and ZrO_2) incorporated

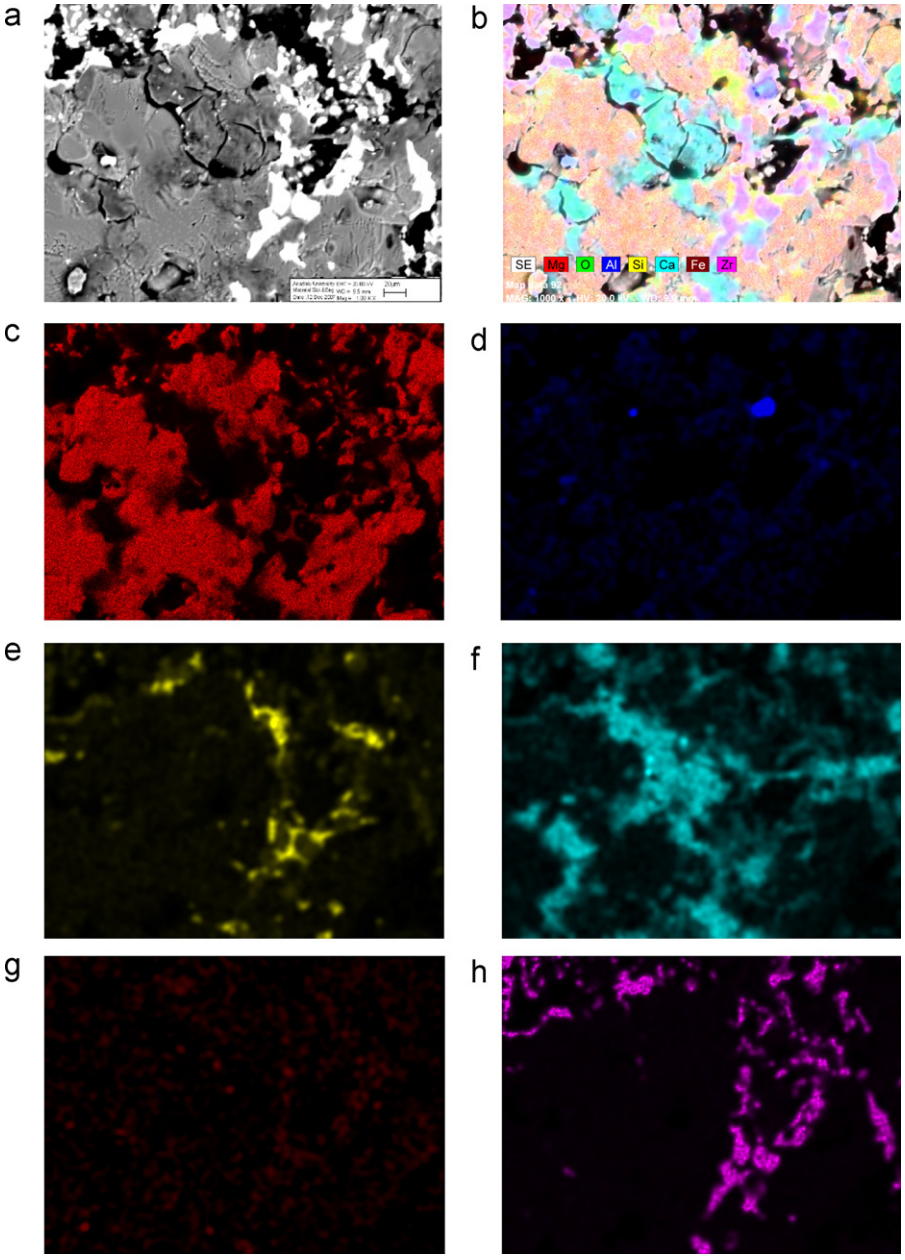

Fig. 9. Microstructural image of a composite refractory having M–5%S–20%ZrO_2 composition (a and b) and distribution of elements [(c) Mg, (d) Al, (e) Si, (f) Ca, (g) Fe, and (h) Zr].

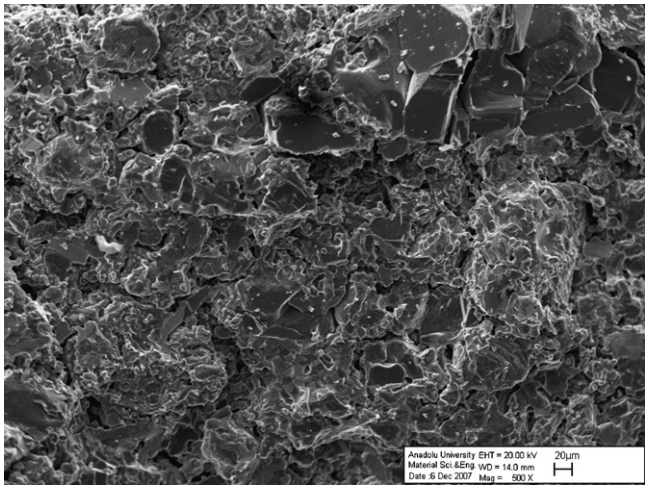

Fig. 10. Fracture surface image of a material with composition of M–5%S–20%ZrO_2.

into MgO were increased, the grain size of composites decreased 1.7-fold, a significant level compared to pure MgO. Fig. 9 shows that when ZrO_2 particles were located among the MgO grains, no grain growth occurred in M–S–ZrO_2 composites as it was observed in pure MgO [11,13,14]. As a consequence of the decrease in MgO grain size with the addition of ZrO_2 to M–S in comparison with additive-free MgO [32,33], the shortening of the propagation distance of microcracks formed after sintering is associated with the improvement in the mechanical properties (Fig. 9).

The image of fracture surface of the composite refractory having M–5%S–20%ZrO_2 composition is given in Fig. 10. The analysis of the fracture surfaces of M and M–S materials shows that there are mainly (i) transgranular cracks in MgO and (ii) intergranular cracks in M–S materials [11,13,14,34]. It was observed that compared to the fracture surface images of M–S materials produced with the addition of ZrO_2, mostly intergranular and some transgranular fractures occurred concurrently in the microstructure. While medium-large size MgO grains underwent transgranular fractures, intergranular fractures occurred in zones with fine sized constituents exhibiting more homogeneous distribution. Although additives surrounded MgO grains, medium-large size grains were not affected by the additives since there was no penetration into these grains. Overall; addition of ZrO_2 to M–S was found to be a significant factor affecting mechanical properties and thermal shock behaviour, inducing the above listed microstructural changes.

The R_{st} parameter represents the maximum temperature difference allowed required for propagation of long cracks under severe thermal stress conditions and is used in estimating the further weakening of a composite refractory and crack stability with the increase in the severity of thermal shock [29]. The R_{st} thermal shock parameter values used in determining high temperature performances of composite refractories are given in Fig. 11. R_{st} values of M–S refractories remained at approximately same levels up to the addition of 10% spinel; however, R_{st} parameter increased significantly with the addition

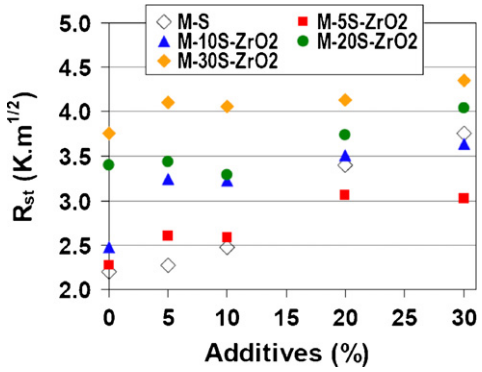

Fig. 11. R_{st} parameter as a function of additives (additives: (i) $MgAl_2O_4$ for M–S and (ii) ZrO_2 for M–S–ZrO_2).

of >10% spinel to MgO. In addition, ZrO_2 incorporation into M–S increased R_{st} data markedly. It was determined that in general, R_{st} values of M–S–ZrO_2 composite refractories were significantly higher than those of M–S materials. Looking at R_{st} thermal shock parameter values, M–30%S–ZrO_2 composite refractories were identified to be compositions displaying high resistance against thermal shocks, with maximum levels of improvement. Additions of (i) 5%ZrO_2 to M–30%S and (ii) 30%ZrO_2 to M–30%S leading to a significant increase in R_{st} values, as compared to (i) M–5%S and (ii) M–30%S compositions, caused 1.8-fold and 1.2-fold improvements, respectively (Fig. 11). In general, R_{st} values are fully consistent with the mechanical properties and specifically the fracture surface energy values. Comparison of the amounts of incorporated additives shows that M–30%S–5%ZrO_2 composition was the material, which displayed the optimum crack stability with the increase in thermal shock severity, showing 1.8-fold maximum resistance against the propagation of long cracks under severe thermal stress conditions and further weakening of the body.

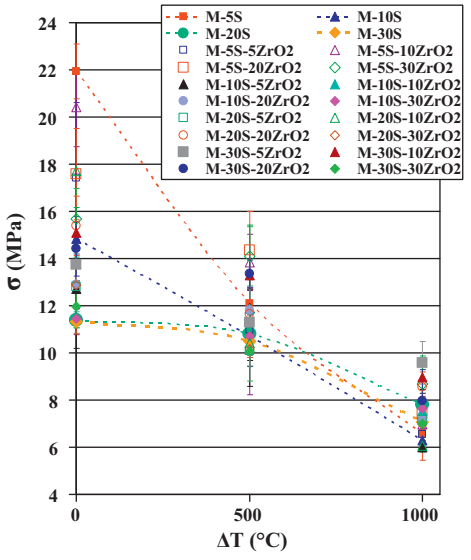

Fig. 12. Strength (σ) values of M–S and M–S–ZrO_2 composite refractories containing varying quantities of additives as a function of thermal shock temperatures (additives: (i) $MgAl_2O_4$ for M–S and (ii) ZrO_2 for M–S–ZrO_2).

Strength values measured after performing thermal shock tests of composite refractory materials were determined as a function of thermal shock temperature (Fig. 12). Strength values exhibited a periodical decrease with increasing thermal shock temperature. Strength data measured at 500 and 1000 °C thermal shock temperatures were examined. In these temperature ranges, some of the M–S–ZrO_2 compositions have similar strength values to M–S materials; however, the great majority of M–S–ZrO_2 compositions have overall much higher strength values than that of M–S composites. In general, thermal shock test results display a similar trend with mechanical properties and R_{st} parameter data and thermal shock results verify R_{st} values. Therefore, R_{st} thermal shock parameter was determined to be a reliable indicator, which may be used in determining the thermal shock resistance of composite refractories.

Materials with the highest strength values among M–S composite refractories produced by incorporating varied ratios of ZrO_2, for which thermal shock tests were performed, were determined to be (i) at 500 °C, M–5%S–20%ZrO_2 and (ii) at 1000 °C, M–30%S–5%ZrO_2 compositions (Fig. 12). It was found that when M–5%S–20%ZrO_2 containing composite was compared to M–S materials showing maximum and minimum thermal shock resistances, (i) M–5%S and (ii) M–30%S; the specified material thermally quenched at 500 °C had (i) 1.19-fold and (ii) 1.37-fold higher thermal shock resistance, respectively. Furthermore, it was determined that when composites were exposed to maximum thermal shock temperature at 1000 °C, the refractory having M–30% S–5%ZrO_2 composition had (i) 1.23-fold and (ii) 1.52-fold higher thermal shock resistance respectively when compared with (i) M–20%S and (ii) M–10%S materials among M–S compositions that had maximum and minimum thermal shock resistance. It was also stated that the addition of 5%ZrO_2 to M–30%S improved the thermal shock resistance by a factor of 1.36 among the materials thermally shocked at 1000 °C. MgO–spinel–ZrO_2 refractories used at high temperatures showed a low strength loss with a high thermal shock damage resistance, leading to a longer service life for industrial uses.

4. Conclusions

An improvement in general reaching and exceeding ∼1.5-fold was observed in the mechanical properties and R_{st} values of composite refractories produced by adding ZrO_2 to M–S. Improvement reaching 1.5-fold was observed as a result of the thermal shock tests with the obtained results verifying the R_{st} parameter data. Therefore, R_{st} parameter was determined to be a reliable indicator, which may be used in determining the thermal shock resistance of M–S–ZrO_2 composite refractories. At tested thermal shock temperatures; at 1000 °C, M–30%S–5%ZrO_2 and at 500 °C, M–5%S–20%ZrO_2 were identified to be compositions exhibiting maximum thermal shock resistance. The basic parameters in the improvement of the mechanical and thermal shock behaviour of composites having M–S–ZrO_2 composition were in general determined to be as follows: (i) propagation of the microcracks formed in the structure for a short distance by interlinking to each other, (ii) arresting or deviation of microcracks when coming across ZrO_2 particles or reaching pores, (iii) concurrent occurrence of mostly intergranular and some transgranular types of fracture on fracture surfaces, and with the incorporation of ZrO_2 (iv) the increase in bulk density, and (v) a significant reduction in MgO grain size. These improvements observed in the thermo-mechanical properties verify that M–S–ZrO_2 composite refractories exhibit a low loss of strength and high thermal shock damage resistance at high temperatures; therefore, leading to a longer service life for using industrial applications.

Acknowledgements

This study was partly supported by Anadolu University and in part TUBITAK under project no: 106M394 with partial support provided also by Konya Selcuklu Krom Magnezit Tugla Sanayi A.S. We would like to express our gratitude to A. Ozkaymak, R. Ozbasi, O. Bezirci, and all agency employees and personnel involved in this project for their support. We also thank the agencies and plant authorities for the supplied equipments and raw materials.

References

[1] R.D. Maschio, B. Fabbri, C. Fiori, Industrial applications of refractories containing magnesium aluminate spinel, Ind. Ceram. 8 (1988) 121–126.
[2] P. Bartha, Magnesia spinel bricks—properties, production and use, in: X. Zhong, et al. (Eds.), Proc. Int. Symp. Refractories, Refractory Raw Materials and High Performance Refractory Products, Pergamon, Hangzhou, 1989, pp. 661–674.
[3] A. Ghosh, R. Sarkar, B. Mukherjee, S.K. Das, Effect of spinel content on the properties of magnesia–spinel composite refractory, J. Eur. Ceram. Soc. 24 (2004) 2079–2085.
[4] G.R. Eusner, D.H. Hubble, Technology of spinel bonded periclase brick, J. Am. Ceram. Soc. 43 (1960) 292–296.
[5] R.M. Evans, Magnesia–alumina spinel raw materials production and preparation, Am. Ceram. Soc. Bull. 72 (1993) 59–63.
[6] D.J. Bray, Toxicity of chromium compounds formed in refractories, Bull. Am. Ceram. Soc. 64 (1985) 1012–1016.
[7] K. Tokunaga, H. Kozuka, T. Honda, F. Tanemura, Further improvements in high temperature strength, coating adherence, and corrosion resistance of magnesia–spinel bricks for rotary cement kiln, in: Proc UNITECR'91 Congress, Aachen, Germany, 1991, pp. 431–435.
[8] C. Aksel, B. Rand, F.L. Riley, P.D. Warren, Thermal shock behaviour of magnesia–spinel composites, J. Eur. Ceram. Soc. 24 (2004) 2839–2845.
[9] R. Sarkar, H.S. Tripathi, A. Ghosh, Reaction sintering of different spinel compositions in the presence of Y_2O_3, Mater. Lett. 58 (2004) 2186–2191.
[10] R. Sarkar, S.K. Das, G. Banerjee, Effect of additives on the densification of reaction sintered and presynthesised spinels, Ceram. Int. 29 (2003) 55–59.
[11] C. Aksel, F.L. Riley, Magnesia–spinel ($MgAl_2O_4$) refractory ceramic composites, in: I.M. Low (Ed.), Ceramic Matrix Composites: Microstructure, Properties and Applications, Woodhead Publishing Limited and CRC Press LLC, USA, 2006, pp. 359–399.
[12] C. Aksel, P.D. Warren, Work of fracture and fracture surface energy of magnesia–spinel composites, Compos. Sci. Technol. 63 (2003) 1433–1440.
[13] C. Aksel, B. Rand, F.L. Riley, P.D. Warren, Mechanical properties of magnesia–spinel composites, J. Eur. Ceram. Soc. 22 (2002) 745–754.
[14] R. Ceylantekin, The effects of $ZrSiO_4$ and ZrO_2 additions on mechanical, thermal shock and corrosion behaviours of MgO–$MgAl_2O_4$ refractories, PhD thesis, Anadolu University, Main Scientific Discipline: Ceramic Engineering, Eskisehir, Turkey, 2009.

[15] BS 7134, Methods for determination of density and porosity, in: British Standard Testing of Engineering Ceramics, Part 1, Section 1.2, 1989.
[16] ASTM C1161-90, Standard test method for flexural strength of advanced ceramics at ambient temperature, Annual Book of ASTM Standards, vol. 15.01, ASTM, 1991, pp. 327–333.
[17] ASTM D790M-86, Standard test methods for flexural properties of unreinforced and reinforced plastics and electrical insulating materials, Annual Book of ASTM Standards, vol. 08.01, ASTM, 1988, pp. 290–298.
[18] D.R. Larson, J.A. Coppola, D.P.H. Hasselman, Fracture toughness and spalling behaviour of high-Al_2O_3 refractories, J. Am. Ceram. Soc. 57 (1974) 417–421.
[19] ASTM E399-90, Standard test method for plane-strain fracture toughness of metallic materials, Annual Book of ASTM Standards, vol. 03.01, ASTM, 1991, pp. 485–515.
[20] ASTM D5045-91, Standard test methods for plane-strain fracture toughness and strain energy release rate of plastic materials, Annual Book of ASTM Standards, vol. 08.03, ASTM, 1991, pp. 728–736.
[21] W.F. Brown, J.E. Srawley, Plane strain crack toughness testing of high strength metallic materials, in: ASTM Special Technical Publication No. 410, 1967.
[22] A.A. Griffith, The theory of rupture, in: Proceedings of the First International Congress for Applied Mechanics, 1924, pp. 55–63.
[23] A.A. Griffith, The phenomena of rupture and flow in solids, Philos. Trans. R. Soc. A221 (1920) 163–198.
[24] R.A. Sack, Extension of Griffith's theory of rupture to three dimensions, in: Proc. Physical Soc., vol. 58, London, (1946), pp. 729–736.
[25] R.W. Davidge, Mechanical Behaviour of Ceramics, Cambridge University Press, Cambridge, 1979.
[26] R. Morrell, Handbook of Properties of Technical and Engineering Ceramics, Part 1, Her Majesty's Stationery Office, London, 1985.
[27] C. Aksel, F.L. Riley, Effect of particle size distribution of spinel on the mechanical properties and thermal shock performance of MgO–spinel composites, J. Eur. Ceram. Soc. 23 (2003) 3079–3087.
[28] M.I. Mendelson, Average grain size in polycrystalline ceramics, J. Am. Ceram. Soc. 52 (1969) 443–446.
[29] D.P.H. Hasselman, Thermal stress resistance parameters for brittle refractory ceramics: a compendium, Am. Ceram. Soc. Bull. 49 (1970) 1033–1037.
[30] J.F. Shackelford, W. Alexander, J.S. Park (Eds.), CRC Materials Science and Engineering Handbook, CRC Press, Boca Raton, FL, 1994.
[31] S.J. Burnett, Properties of Refractory Materials, UKAEA Research Group Report, Harwell, 1969.
[32] M. Chen, C. Lu, J. Yu, Improvement in performance of MgO–CaO refractories by addition of nano sized ZrO_2, J. Eur. Ceram. Soc. 27 (2007) 4633–4638.
[33] P.G. Lampropoulou, C.G. Katagas, Effects of zirconium silicate and chromite addition on the microstructure and bulk density of magnesia–magnesium aluminate spinel based refractory materials, Ceram. Int. 34 (2008) 1247–1252.
[34] C. Aksel, P.D. Warren, F.L. Riley, Fracture behaviour of magnesia and magnesia–spinel composites before and after thermal shock, J. Eur. Ceram. Soc. 24 (2004) 2407–2416.